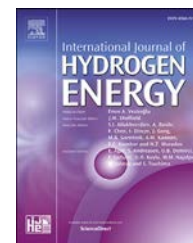


Available online at www.sciencedirect.com

ScienceDirect

journal homepage: www.elsevier.com/locate/hj

A first principles study of hydrogen storage in lithium decorated defective phosphorene

Sandip Haldar ^a, Sankha Mukherjee ^a, Farheen Ahmed ^a,
Chandra Veer Singh ^{a,b,*}

^a Department of Materials Science and Engineering, University of Toronto, Toronto, ON, M5S 3E4, Canada

^b Department of Mechanical and Industrial Engineering, University of Toronto, Toronto, ON, M5S 3E4, Canada

ARTICLE INFO

Article history:

Received 1 May 2017

Received in revised form

17 July 2017

Accepted 18 July 2017

Available online 10 August 2017

Keywords:

Phosphorene

Hydrogen storage

Lithium decoration

Density functional theory

ABSTRACT

In this study, we studied defect-engineering and lithium decoration of 2D phosphorene for effective hydrogen storage using density functional theory. Contrary to graphene, it is found that the presence of point-defects is not preferable for anchoring of H_2 molecules over defective phosphorene. According to previous research, strategies such as defect engineering, metal decoration, and doping enhance the hydrogen storage capacity of several 2D materials. Our DFT simulations show that point defects in phosphorene do not improve the hydrogen storage capacity compared to pristine phosphorene. However, selective lithium decoration over the defective site significantly improves the hydrogen adsorption capacity yielding a binding energy of as high as -0.48 eV/ H_2 in Li-decorated single vacancy phosphorene. Differential charge densities and projected density of states have been computed to understand the interactions and charge transfer among the constituent atoms. Strong polarization of the H_2 molecule is evidenced by the charge accumulation and depletion. The PDOS shows that the presence of Li leads to enhanced charge transfer. The maximum gravimetric density was investigated by sequentially adding H_2 molecules to the Li-decorated single vacancy defective phosphorene. The Li-decorated single vacancy phosphorene is found to possess a gravimetric density of around 5.3% for hydrogen storage.

© 2017 Hydrogen Energy Publications LLC. Published by Elsevier Ltd. All rights reserved.

Introduction

Hydrogen fuel has attracted increased attention as a source of clean energy in order to tackle the adverse environmental issues of fossil fuels due to carbon emission. Fossil fuel based energy systems produce pollutants in greater amounts and are more damaging than those produced by renewable hydrogen energy systems. In fact, an engine that burns pure hydrogen produces almost no environmental pollution [1].

Therefore, hydrogen based energy systems are promising for solving environmental problems and the energy crisis [2]. Significant research effort is being invested in developing safe, cost-effective and efficient hydrogen storage media for fuel cell applications [3]. Barthelemy et al. [4] have reviewed the industrial perspective of H_2 fuel cells in the light of the H_2 fuel market with applications as fuel in transportation and stationary power sources.

One of the primary concerns of using H_2 fuel as a practical alternative to fossil fuels is its storage and handling.

* Corresponding author. Department of Materials Science and Engineering, University of Toronto, Toronto, ON, M5S 3E4, Canada.

E-mail address: Chandraveer.Singh@utoronto.ca (C.V. Singh).

<http://dx.doi.org/10.1016/j.ijhydene.2017.07.143>

0360-3199/© 2017 Hydrogen Energy Publications LLC. Published by Elsevier Ltd. All rights reserved.

Conventional methods to store H_2 use high pressure gas cylinders (up to 800 bar) or as liquid H_2 in cryogenic tanks (at 21 K) [5]. However, these methods are inefficient and unsafe for automotive applications. In order to achieve efficient and safe storage, H_2 adsorption into substrates with a high specific surface area is a promising route [5,6]. Effective H_2 storage based on physisorption mechanism requires: (a) a high gravimetric density: a target of 7.5 wt % system gravimetric density was decided as revised target the United States Department of Energy (USDOE) [7] for ultimate full fleet applications, and (b) easy recycling of hydrogen at ambient pressure and temperature [8,9]. While experimental studies are costly, computational investigations have emerged as a viable avenue to determine the performance of a potential host substrate for H_2 storage. In the past, density functional theory (DFT) calculations were extensively used to investigate the possibility and capacity of a material for effective H_2 storage. The leading parameter to identify the potential of a material for H_2 storage is its binding energy that should be in the range of between 0.2 and 0.6 eV/ H_2 for reversible H_2 storage (i.e. adsorption and release at near ambient conditions) [10]. The maximum gravimetric density can be predicted by sequential adsorption of H_2 molecules and relating it to the binding energy of the system.

Several materials have been demonstrated to be potential substrates for H_2 storage, e.g. metal organic frameworks [11], covalent-organic frameworks [12], carbon nanotubes [13], boron nitride sheets [14] and fullerenes [15–17]. 2D materials, by virtue of their high surface area to volume ratio, offer greater benefits for H_2 storage. With the advent of nanotechnologies, unprecedented advances are being made in fabricating new 2D materials [18,19]. In recent years, several 2D materials have been demonstrated to be potential substrates for H_2 storage, e.g. metal decorated pristine graphene has shown great promise as a potential candidate for H_2 adsorption and efficient storage [20]. Recently, Li-decorated porous graphene and naphthalene were investigated as potential substrate for H_2 storage [21,22]. It was found that metal decoration enhances the capacity of H_2 storage of the substrate. Nevertheless, it is also well known that the adsorption of metallic atoms over pristine graphene is rather weak with binding energies to the tune of 0.6 eV/ H_2 and as a result, metallic adatoms tend to cluster over the graphene substrate [23].

Phosphorene, a new p-type semiconducting 2D material of phosphorous, has been fabricated recently [24,25]. Phosphorene is unique compared to graphene because of its layer-dependent bandgap which ranges between 0.3 eV (bulk) and 1.5 eV (monolayer), and therefore, has the capacity to perform in applications where gapless graphene and large band gap transition metal dichalcogenides (TMDSs) cannot cater to [24]. Phosphorene has a six-ringed structure, however, unlike graphene, it has a puckered structure due to sp^3 hybridized P–P bonds resulting in a higher surface-area-to-volume ratio [26,27]. Moreover, although heavier than graphene, monolayer black phosphorous (MBP) is lighter than most of the known 2D materials [27] and can be exfoliated mechanically [28]. Recent research articles have demonstrated phosphorene to be promising in several applications, e.g. nanoelectronics, optoelectronics and photovoltaics [25,29–31]. Additionally,

phosphorene has been recently investigated to evaluate its capability to adsorb metals [32], nonmetals [33], small molecules [34] and H_2 [27,35]. Li et al. [27] have shown that pristine phosphorene is a rather weak substrate for the adsorption of H_2 molecules with a binding energy of 0.07 eV/ H_2 , however, Li-decoration increased the binding energy to 0.18 eV. Yu et al. [35] reported that the phosphorene structures used by Li et al. [27] were unstable, and the gravimetric density in Li-decorated pristine phosphorene was limited to 4.4% [35].

We utilized defect engineering and Li-decoration to enhance the H_2 storage capacity of phosphorene. Li adatoms were selected owing to their light weight, which enhances the gravimetric density of the system and that it binds strongly with defective phosphorene substrates [36]. Previous researches also indicate that metallic adatoms tend to cluster on defect free substrates instead of homogeneously dispersing owing to their large cohesive energy [37,38]. This phenomenon severely limits the hydrogen storage performance of metal-decorated 2D materials. One way of tackling this problem is to introduce lattice defects in the substrate which would enhance the bond strength between the metallic adatom and the substrate, thereby inhibiting clustering of the adatoms [39,40]. This method is advantageous because lattice defects are inadvertently created during the synthesis of 2D materials. On the other hand, increased interaction between the adatom and the substrate reduces the amount of charge available to facilitate the interactions with the H_2 molecules [41]. Therefore, we must find structural defects that would prevent clustering of adatoms without negotiating with large and efficient H_2 storage. Three defects, namely single vacancy (SV), double vacancy (DV) and Stone-Wales (SW) were considered as they are relatively stable and possess low formation energies [42]. In order to gain further insight into H_2 adsorption onto defective phosphorene, differential charge density (DCD) and projected density of states (PDOS) were computed.

Material and computational detail

Plane wave pseudopotential based DFT calculations were performed using the open source package Quantum Espresso available under the GNU license [43]. For the DFT calculations, Perdew-Burke-Ernzerhof (PBE) exchange correlation functional [44] and Martins-Troullier NORMCONS type pseudopotential [45] in semilocal form generated by scalar relativistic calculation were used with Van der Waals correction in the dispersion corrected DFT (DFT-D) framework. In the DFT-D method, the van der Waals correction depends only on the positions of the nuclei and the exchange correlation functional and describes the nonlocal dispersion effects more accurately [46,47]. To avoid any inter-layer interactions between phosphorene surfaces from long-range van der Waals forces due to periodicity, we used a vacuum spacing of 20 Å. The cutoff energy for wave function expansion was set at 60 Ry (1 Ry = 13.61 eV) and that of the charge density was set at 480 Ry. Brillouin zone integrations were performed using a Monkhorst-Pack grid with $4 \times 4 \times 1$ k-points [48]. The Methfessel–Paxton smearing with a degauss value of 0.02 was used in the simulations [49]. The binding energy of H_2 for each case can be calculated as:

$$E_b = (E_{\text{phos+iH}_2} - E_{\text{phos}} - E_{\text{iH}_2})/i, \quad (1)$$

$$E_b = (E_{\text{phos+Li+iH}_2} - E_{\text{phos+Li}} - E_{\text{iH}_2})/i, \quad (2)$$

where E_b represents the average binding energy of the hydrogen and $E_{\text{phos+iH}_2}$, E_{phos} , E_{iH_2} are the total energy of phosphorene and $i\text{H}_2$ molecules, only phosphorene, and only $i\text{H}_2$ molecules, respectively. Similarly, $E_{\text{phos+Li+iH}_2}$ and $E_{\text{phos+Li}}$ represent the total energy of the full Li-decorated H_2 -adsorbed phosphorene, and Li-decorated phosphorene, respectively. As per our definition, a negative binding energy implies that the adsorption is energetically favorable and occurring, while a positive binding energy indicates no adsorption. Smaller values of E_b imply a stronger binding of the H_2 with the substrate.

In order to compute the charge density, self consistent field (SCF) calculations were performed using a convergence threshold of $1e^{-5}$ Ry for the total system energy. The charge density differences ($\Delta\rho$) have been computed using the relations:

$$\Delta\rho = \rho_{\text{phos+iH}_2} - \rho_{\text{phos}} - \rho_{\text{iH}_2}, \quad (3)$$

$$\Delta\rho = \rho_{\text{phos+Li+iH}_2} - \rho_{\text{phos+Li}} - \rho_{\text{iH}_2}, \quad (4)$$

where $\rho_{\text{phos+iH}_2}$, ρ_{phos} , and ρ_{iH_2} represent the charge density of phosphorene and $i\text{H}_2$ molecules, only phosphorene, and $i\text{H}_2$ molecules, respectively. For the Li decorated system, $\rho_{\text{phos+Li+iH}_2}$ and $\rho_{\text{phos+Li}}$ represent the charge densities of Li-decorated phosphorene substrate with adsorbed H_2 molecules and only Li-decorated phosphorene substrate, respectively.

At first, the defective phosphorene substrates were relaxed at their ground state. DFT calculations were performed with several initial positions of the H_2 molecule, and the smallest

binding energies are reported here. In order to study the effect of Li-decoration, the Li atom was adsorbed over the defective phosphorene substrate. The Li-decoration was performed by choosing the favorable sites for Li, following the literature [36]. H_2 molecules were then added to the supercell and stabilized energetically.

Results and discussions

As a benchmark, the binding energy associated with the adsorption of a H_2 molecules on defective phosphorene substrates (with and without Li decoration) are compared with that of pristine phosphorene which has been reported to be -0.07 eV [27].

Defective phosphorene

Similar to graphene, phosphorene is known to have stable structures with single vacancy (SV), double vacancy (DV) and Stone Wales (SW) defects as evidenced by their lower formation energies [42]. In this work, these three defects, i.e. SV, DV and SW were considered in order to study the H_2 storage capacity by defect engineering. Initially, when the pristine phosphorene supercell was created, the lattice parameters of pristine phosphorene were obtained to be 4.62 \AA in the armchair direction and 3.30 \AA in the Zigzag direction respectively. The defective phosphorene substrates were then relaxed at their ground state by energy minimization. Following the work by Zhang et al. [36], who have studied the stability and kinetics of a host of point defects in monolayer phosphorene, energetically stable single and double vacancy phosphorene substrates were created by removing P atoms from their lattice positions and Stone-Wales defect by rotating a P–P bond by 90° with regard to the midpoint of the bond.

The formation energies of the defective phosphorene have been calculated using the relation [36],

$$E_f = E_{\text{defect}} - \frac{N-n}{N} E_{\text{pristine}}, \quad (5)$$

where E_{defect} , E_{pristine} are the total energies of the defective and defect-free (pristine) phosphorene, respectively, N is the number of atoms in the pristine unit cell, and n is the number of atoms removed from the pristine cell to create the defect ($n=1$ for SV and SW, and $n=2$ for DV). As summarized in Table 1, the calculated formation energies for the DV 5-8-5, SV

Table 1 – Formation energies for different defects in phosphorene and those reported in literature and comparison with those of graphene.

Phosphorene Defect	Graphene [50,51]			
	E_f (eV)	Zhang et al. [36]	Hu and Yang [42]	
SV	1.71	1.29	1.62	7.38–7.85
DV	1.46	1.28	1.90	7.52–8.70
SW	1.11	1.63	1.01	4.50–5.30

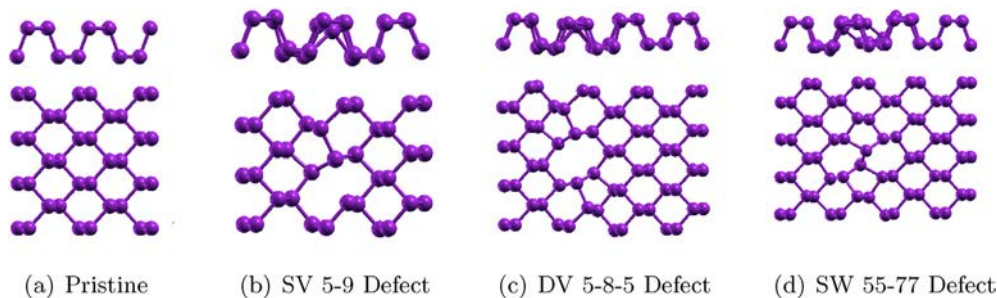


Fig. 1 – Schematic models of Pristine, Single vacancy (SV), Double vacancy (DV) and Stone Wales (SW) defective phosphorene.

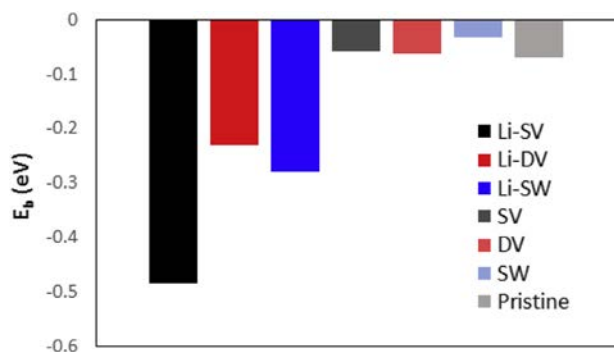


Fig. 2 – Binding energies (E_b) of H_2 molecules for pristine [27], Single Vacancy (SV), Double Vacancy (DV), and Stone Wales (SW) defective phosphorene and Li-decorated defective phosphorene substrates.

Table 2 – Binding energy ($E_b^{H_2}$), perpendicular height (Z) from substrate, and bond length (R) of H_2 and binding energy of Li (E_b^{Li}) in different defective and Li-decorated defective phosphorene. The binding energies correspond to adsorption of one H_2 molecule. The perpendicular height is measured from the closest phosphorous atom in defective phosphorene and from Li atom in Li-decorated defective phosphorene.

System	$E_b^{H_2}$ (eV)	Z (Å)	R (Å)	E_b^{Li} (eV)
SV	-0.058	2.02	0.745	–
DV	-0.062	2.95	0.746	–
SW	-0.031	2.27	0.744	–
SV-Li	-0.48	1.82	0.750	-3.21
DV-Li	-0.23	1.88	0.751	-3.02
SW-Li	-0.28	1.82	0.750	-2.49

5-9, and SW 55-77 defects are 1.46 eV, 1.71 eV, and 1.11 eV, respectively. These magnitudes of defect formation energies are in-sync with those reported in literature (Table 1). The formation energies for SV, DV and SW defective phosphorene are listed in Table 1 and are compared to those reported in

literature. For comparison, the formation energies of graphene from literature are also listed. It can be noted that formation of defects in phosphorene is easier than in graphene. The optimized structure of these point defects in phosphorene obtained from our DFT simulations are shown in Fig. 1.

H_2 adsorption on defective phosphorene

The binding energies obtained by using Eq. (1), are presented in Fig. 2. These values are also presented in Table 2 along with the distance between the H_2 molecule and the nearest phosphorous atom in the relaxed structure. It is observed that, among the defective phosphorene substrates, the DV phosphorene has the best binding energy (-0.062 eV/ H_2), which is well above the acceptable limit for effective H_2 storage. In order to showcase the interaction between the H_2 molecule and the phosphorene substrates, the differential charge density (DCD) and partial density of state (PDOS) are depicted in Figs. 3 and 4. It can be noted from the charge density difference plots that the charges are spread apart from the H_2 molecules indicating interactions between the substrates and the H_2 molecules. The change in the PDOS of electrons in the p shell of the H_2 -adsorbed defective phosphorene as compared to that in the phosphorene substrate without H_2 shows the charge transfer from the H_2 molecules to the substrates (Fig. 4(a)). The PDOS of the s electron in H_2 reduces after adsorption as compared to that of only H_2 (Fig. 4(b)).

H_2 adsorption on Li-decorated defective phosphorene

DFT simulations of H_2 adsorption onto Li decorated defective phosphorene were performed to evaluate the effects of Li decoration onto H_2 adsorption. At first Li atoms were adsorbed over the defective phosphorene substrates by choosing favorable sites reported previously. H_2 molecules were then added to the supercell and stabilized energetically. Similar to literature, in our simulations, enhanced interactions were also observed between Li adatoms and the defective phosphorene substrates. For example, the binding energies

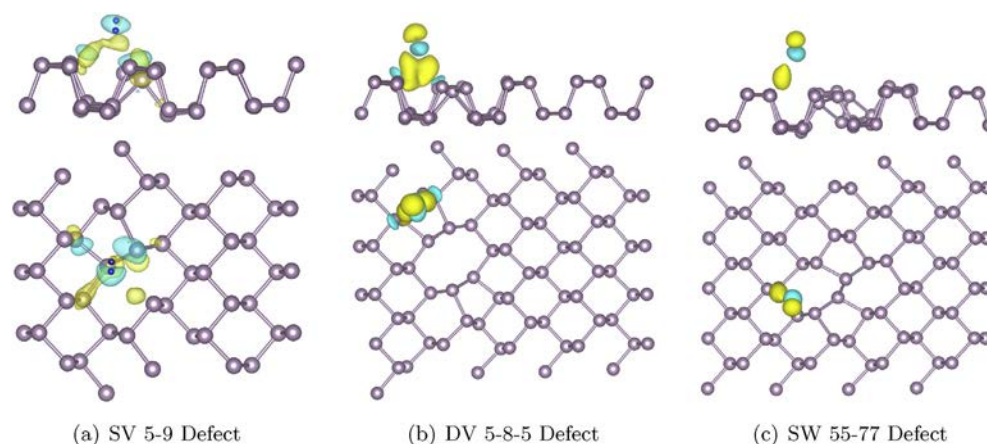


Fig. 3 – Differential Charge Densities (DCDs) of in H_2 adsorbed (a) SV 5-9, b (b) DV 5-8-5, and (c) SW 55-77 phosphorene. The P and H atoms are represented by violet and blue spheres. Yellow and light blue regions indicate charge accumulation and depletion, respectively. The isosurface level is set to be $9e^{-5}$ e \AA^{-3} for (a) SV, (b) DV and (c) SW. (For interpretation of the references to colour in this figure legend, the reader is referred to the web version of this article.)

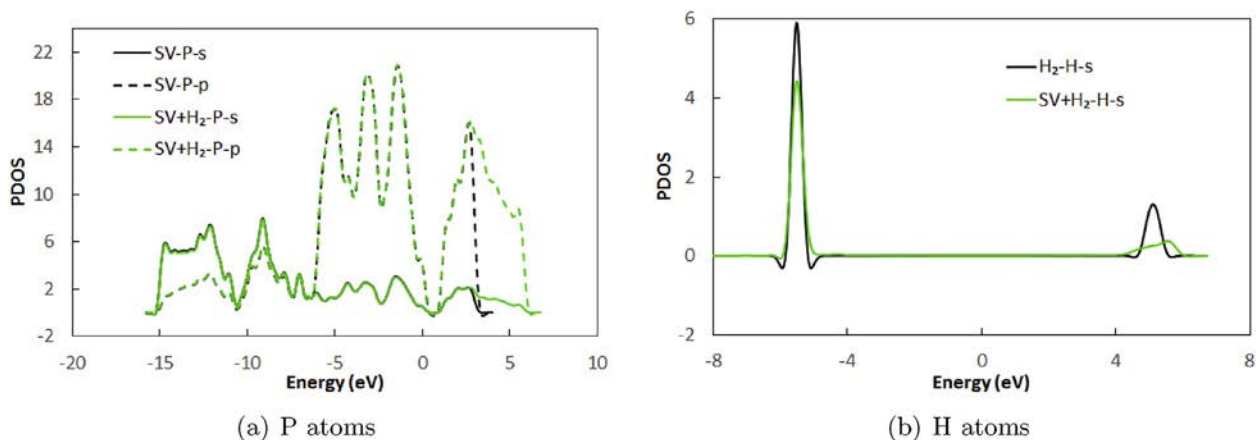


Fig. 4 – PDOS of (a) P and (b) H atoms before and after H_2 adsorption with Fermi energy shifted to zero. SV represents only SV phosphorene, H_2 represents only H_2 , and SV+ H_2 represents SV phosphorene and H_2 .

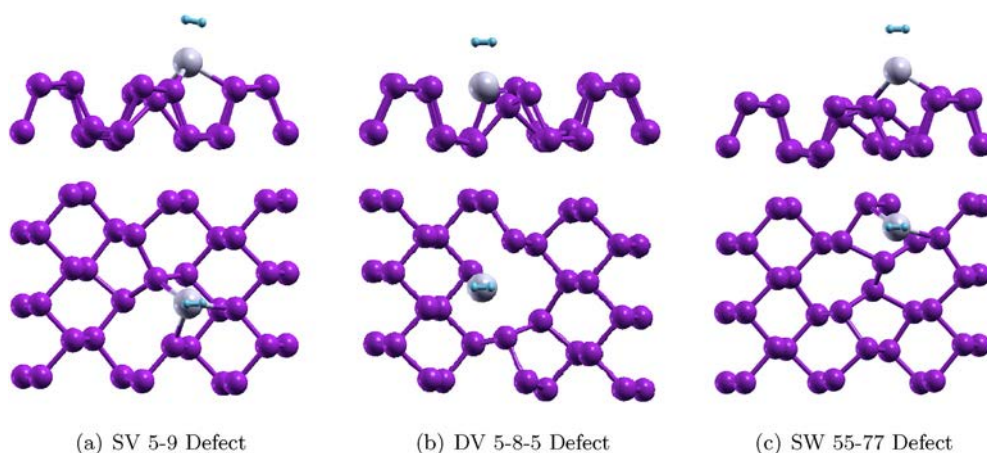


Fig. 5 – Schematic models of Li-decorated SV, DV and SW defective phosphorene.

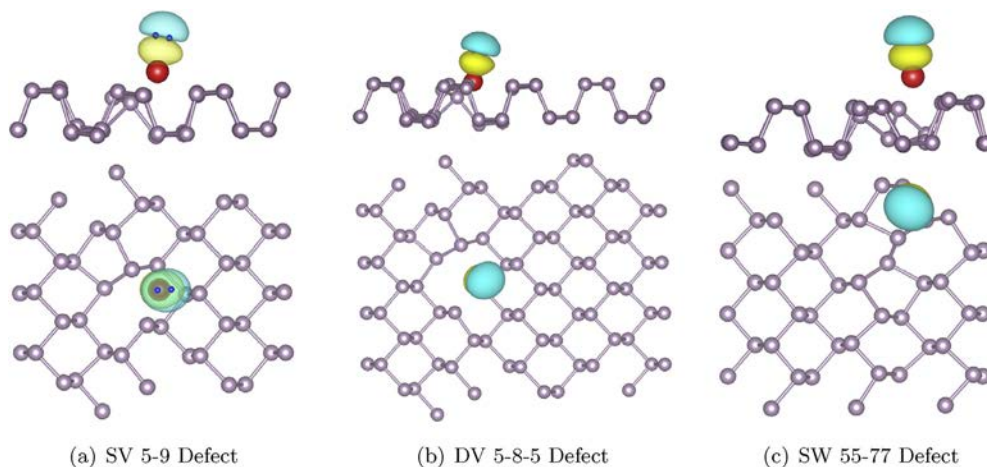


Fig. 6 – Differential Charge Densities (DCDs) in H_2 adsorbed Li-decorated defective phosphorene. The red sphere represents Li atom and dark blue spheres represent H_2 atoms. The isosurface levels are set to $0.00045 \text{ e } \text{\AA}^{-3}$. Yellow and light blue regions indicate charge accumulation and depletion, respectively. (For interpretation of the references to colour in this figure legend, the reader is referred to the web version of this article.)

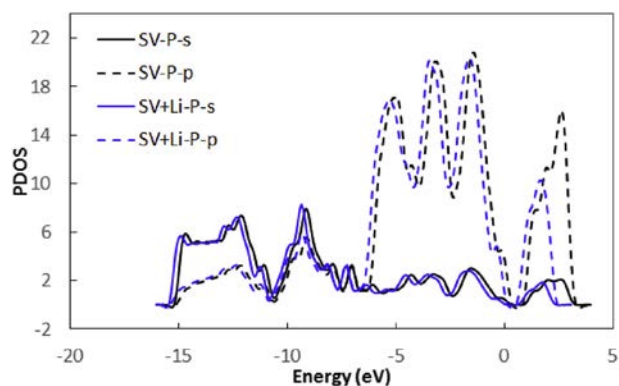


Fig. 7 – PDOS of SV phosphorene (Fermi energy shifted to zero) with and without Li.

of Li adsorption onto SV, DV and SW phosphorene were calculated to be -3.21 eV, -3.02 eV, and -2.49 eV, respectively. These binding energies are much stronger than the cohesive energy of bulk Li. The binding energies of Li adsorption on defective phosphorene are in agreement with previous reports [52]. The atomic configurations of H_2 adsorbed on Li-decorated defective phosphorene are shown in Fig. 5. Following the relaxation of Li-decorated phosphorene, a H_2 molecule was added to the relaxed Li-decorated defective

phosphorene system, in such a way that one of the H atoms in the H_2 molecule faced towards the Li atom in the vertical direction. Our DFT calculations predict that Li-decoration significantly enhances the H_2 adsorption capacity of defective phosphorene. Li-decorated SV defective phosphorene was found to yield the best binding energy (Eq. (2)), as strong as -0.48 eV/ H_2 , and the SW and DV defective phosphorene were predicted to have binding energies of -0.28 eV/ H_2 , and -0.23 eV/ H_2 , respectively (Fig. 2, Table 2). The vertical distance between the H_2 molecules and the Li atoms are also listed in Table 2. It is found that in all the relaxed structures the distance between the H_2 molecules and the Li atoms lie in the range between 1.82 Å and 1.88 Å.

The differential charge densities (DCD) were computed from the DFT results for understanding the charge transfer among different constituent atoms in the presence of Li adatoms (Fig. 6). The DCDs show regions of charge accumulation and depletion on either side of the hydrogen molecules indicating strong polarization of the hydrogen molecules. The charge density suggests that the hydrogen binds by a weak electrostatic dipole mechanism without any strong hybridization or covalent bonding [20]. From these results, we deduce that the H_2 molecules were adsorbed by the Li atom and there were no Kubas interactions [41]. The weaker bonding type is believed to be better in the context of reversible H_2 storage where less energy can activate the release of stored H_2 .

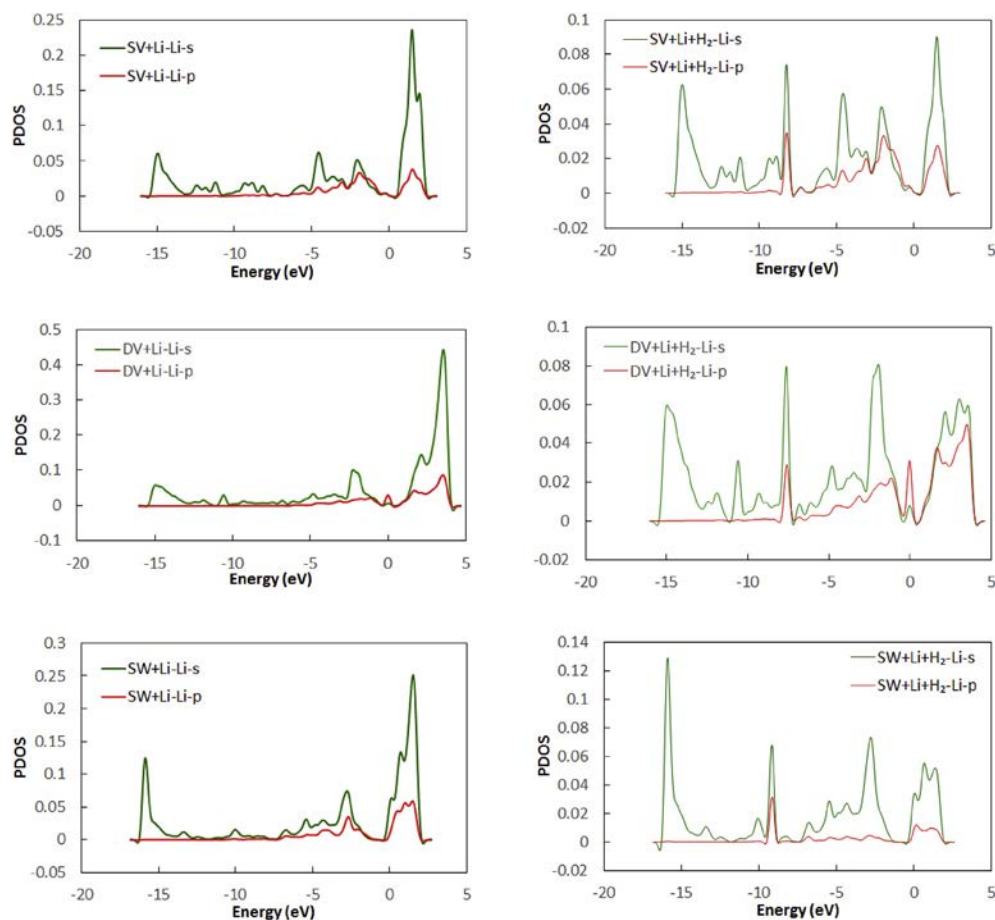


Fig. 8 – PDOS of Li in Li-decorated defective phosphorene (left) before and (right) after H_2 adsorption.

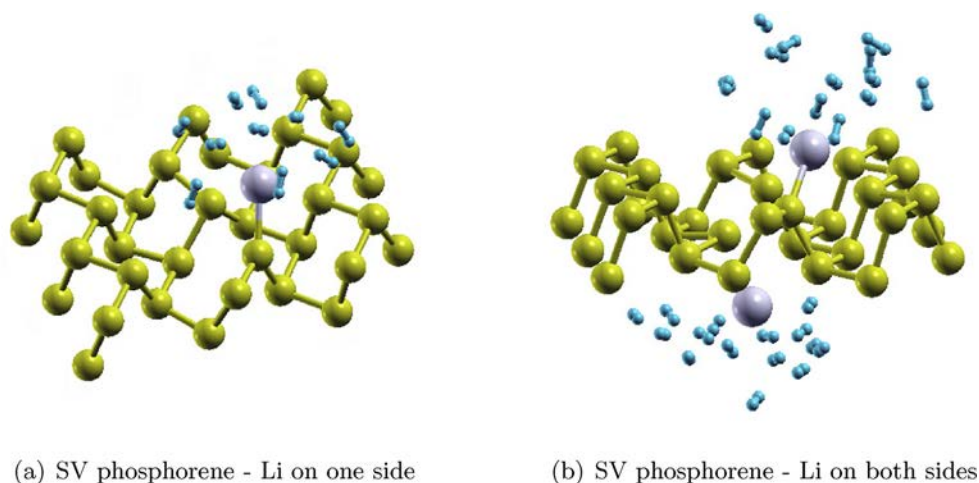


Fig. 9 – SV phosphorene for H_2 storage with Li decoration on (a) one side and (b) both sides.

In order to investigate the effect of Li on the charge transfer mechanism leading to better H_2 adsorption, the projected density of states were compared for SV phosphorene and Li-decorated SV phosphorene. Fig. 7 depicts the total PDOS of s and p shells of electrons in phosphorene with and without Li decoration. It can be seen that the PDOS of p shell electrons in phosphorene is affected (around 3 eV) due to the presence of Li indicating interaction between them. The PDOSs of the valence electrons belonging to Li in Li-decorated defective phosphorene before and after H_2 adsorption are shown in Fig. 8, to understand the charge transfer from the Li atom. A comparison of the PDOSs of Li in defective phosphorene before and after H_2 adsorption shows that the $2s$ and $2p$ orbitals of Li in defective phosphorene have higher peaks as compared to those when H_2 is adsorbed in Li-decorated defective phosphorene, indicating enhanced charge transfer from Li to H_2 . The fact that the intensity of the peaks reduces the most for the SV defected phosphorene and least when interacting with DV defected phosphorene corroborates with the prediction of lowest binding energy in SV defective

phosphorene compared to DV defective phosphorene (Figs. 9 and 10).

Gravimetric density in Li-decorated defective phosphorene

The gravimetric density was calculated in order to estimate the maximum capacity of H_2 storage in Li-decorated SV phosphorene. We focused on SV phosphorene since the Li-decorated phosphorene with SV defect showed the suitable binding energy (Section H_2 adsorption on Li-decorated defective phosphorene). The gravimetric density of H_2 storage is given by

$$C_g = \frac{pm_{H_2}}{qm_p + rm_{Li} + pm_{H_2}}, \quad (6)$$

where m_{H_2} , m_p , m_{Li} and p , q , r represent the atomic mass and number of H_2 , P, and Li, respectively. In order to maximize H_2 adsorption on the phosphorene substrate, it was decorated by two Li atoms on both sides of the substrate followed by H_2 adsorption. To study the gravimetric density, the number of

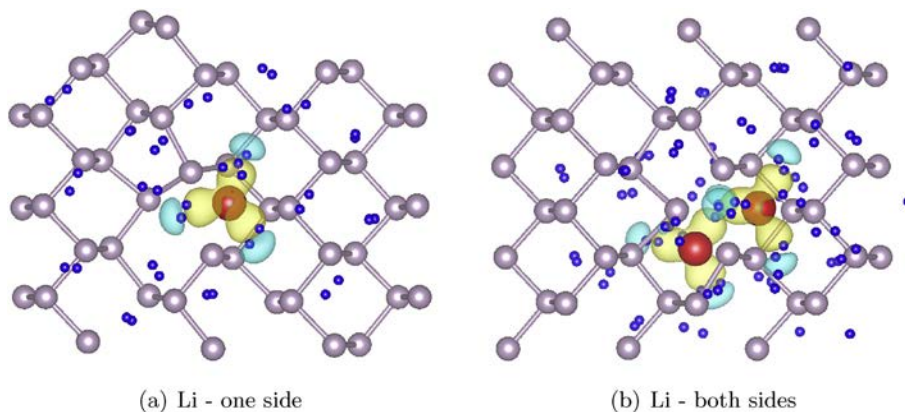


Fig. 10 – Charge density of Li-decorated SV phosphorene. The violet, dark blue and red spheres represent P, H and Li atoms, respectively. The isosurface levels are set to $0.002 \text{ e} \text{ \AA}^{-3}$ to show the charge density differential around the Li atom. Yellow and light blue regions indicate charge accumulation and depletion, respectively. (For interpretation of the references to colour in this figure legend, the reader is referred to the web version of this article.)

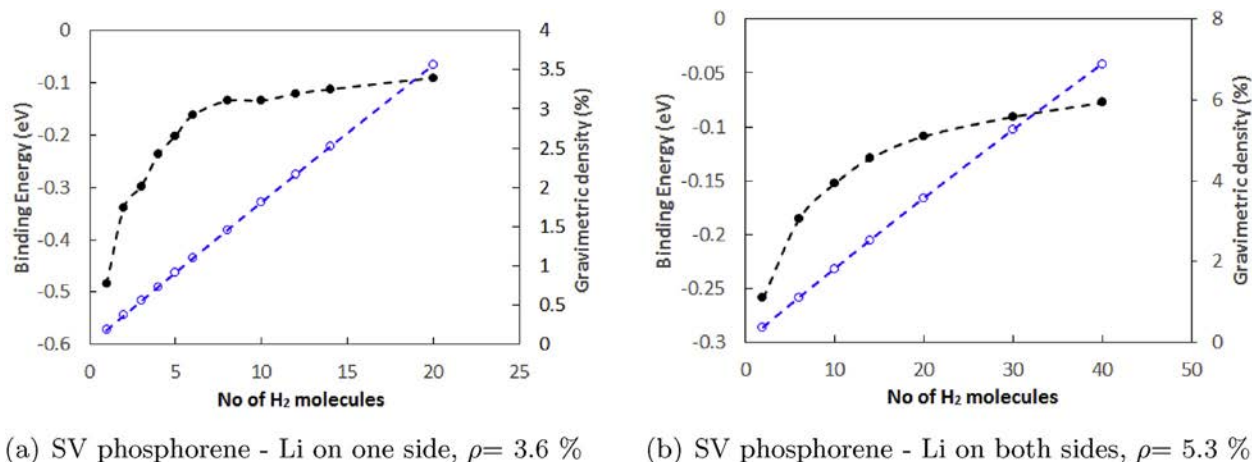


Fig. 11 – Binding energy (black) and gravimetric density (blue) of H₂ adsorption in of Li-decorated SV phosphorene. (For interpretation of the references to colour in this figure legend, the reader is referred to the web version of this article.)

H₂ molecules was sequentially increased and the average binding energy has been computed. It can be noted that after adsorption of the first H₂ molecule, the consequent molecules will have a lesser sequential binding energy as reported by Yu et al. [35]. However, when considering gravimetric density, the average binding energy computed from Eq. (2) is considered following literature [27,35,53]. In both cases (Li atom on one side and both sides), the number of H₂ molecules has been increased till the average binding energy decreased to around -0.1 eV/H₂. It was also noted that the H₂ molecules do not move away from the substrate indicating adsorption to phosphorene. It can be noted that defect density was not varied in this study. The average binding energy and the corresponding gravimetric density of H₂ adsorption over SV phosphorene decorated with one Li atom are depicted in Fig. 11(a) as a function of number of molecules of H₂ adsorbed. Additionally, in Fig. 11(b), the average binding energy and gravimetric density associated with H₂ adsorption for Li decoration on both sides of SV phosphorene are presented. As can be observed from the figures, an increase in the number of H₂ molecules affects the average binding energy, leading to a reduced capability for further adsorption. In case of SV phosphorene decorated with one Li atom (Fig. 11(a)), a gravimetric density of 3.6% was predicted with a binding energy being around -0.1 eV/H₂ ($p=35, q=1, r=20$ in Eq. (6)). Li decoration on both sides of the SV phosphorene substrate (Fig. 11(b)) significantly increased the gravimetric density to 5.3% with a binding energy of around -0.1 eV ($p=35, q=2, r=30$ in Eq. (6)). The gravimetric density of H₂ in metal decorated defective graphene was reported to be 7.02% [54], higher than this, however, it must be noted that the formation energies of the defects in graphene is much higher than those in phosphorene (Table 1).

Conclusions

Density Functional Theory (DFT) calculations were performed to investigate the viability of H₂ storage in defective and Li-decorated defective phosphorene. Three types of

defects, namely the SV 5-9, DV 5-8-5 and SW 55-77, were studied due to their stability and low formation energies. The DFT calculations suggest that the defects in phosphorene do not enhance the H₂ storage capacity compared to that of pristine phosphorene. The binding energies in SV, DV and SW defective phosphorene were computed to be around 0.03 – 0.06 eV/H₂, well below the acceptable range for reversible H₂ storage. Further, the defective phosphorene substrates were decorated with Li atoms, and the capacity of H₂ storage in Li-decorated defective phosphorene substrates was studied. It was observed that Li-decoration in defective phosphorene significantly enhances the H₂ storage, with a binding energy as low as -0.48 eV/H₂ for Li-decorated SV defective phosphorene. DCDs and PDOSs evidence the unique feature of the Li decoration in terms of the charge transfer from Li. The weak bonding of H₂ atoms with the Li-decorated phosphorene makes the H₂ storage and release favorable for effective and reversible H₂ adsorption. In order to study the maximum capacity of H₂ storage, the Li-decorated SV phosphorene (the best case among the three defects) was further investigated by adding more H₂ molecules to determine the binding energy and gravimetric density. To do that, the SV defective phosphorene was decorated with Li on both sides in order to increase the H₂ adsorption capability. A gravimetric density of 3.6% and 5.3% could be achieved by single sided and double sided Li decoration on SV phosphorene, respectively. This is higher than the 4.4% gravimetric density obtained for Li-decorated pristine phosphorene [35] indicating that Li-decoration in defective phosphorene enhances H₂ adsorption better than its pristine counterpart.

Acknowledgments

Computations were performed with support from Compute Canada supercomputing facilities SciNet HPC Consortium [55] and Calcul Qubec. Financial support for this work was provided by Natural Sciences and Engineering Research Council of Canada (NSERC), Connaught New Researcher

Award and the University of Toronto. The authors gratefully acknowledge their support.

REFERENCES

- [1] Momirlan M, Veziroglu TN. The properties of hydrogen as fuel tomorrow in sustainable energy system for a cleaner planet. *Int J Hydrogen Energy* 2005;30(7):795–802.
- [2] Nicoletti G, Arcuri N, Nicoletti G, Bruno R. A technical and environmental comparison between hydrogen and some fossil fuels. *Energy Convers Manag* 2015;89:205–13.
- [3] Muthu RN, Rajashabala S, Kannan R. Hydrogen storage performance of lithium borohydride decorated activated hexagonal boron nitride nanocomposite for fuel cell applications. *Int J Hydrogen Energy* 2017;42:15586–96.
- [4] Barthélémy H, Weber M, Barbier F. Hydrogen storage: recent improvements and industrial perspectives. *Int J Hydrogen Energy* 2017;42(11):7254–62.
- [5] Lim KL, Kazemian H, Yaakob Z, Daud WW. Solid-state materials and methods for hydrogen storage: a critical review. *Chem Eng Technol* 2010;33(2):213–26.
- [6] Züttel A. Materials for hydrogen storage. *Mater today* 2003;6(9):24–33.
- [7] Ao Z, Peeters F. High-capacity hydrogen storage in Al-adsorbed graphene. *Phys Rev B* 2010;81(20): 205406.
- [8] Shevlin S, Guo Z. Density functional theory simulations of complex hydride and carbon-based hydrogen storage materials. *Chem Soc Rev* 2009;38(1):211–25.
- [9] Sahaym U, Norton MG. Advances in the application of nanotechnology in enabling a hydrogen economy. *J Mater Sci* 2008;43(16):5395–429.
- [10] Yoon M, Yang S, Wang E, Zhang Z. Charged fullerenes as high-capacity hydrogen storage media. *Nano Lett* 2007;7(9):2578–83.
- [11] Goldsmith J, Wong-Foy AG, Cafarella MJ, Siegel DJ. Theoretical limits of hydrogen storage in metal–organic frameworks: opportunities and trade-offs. *Chem Mater* 2013;25(16):3373–82.
- [12] Ke Z, Cheng Y, Yang S, Li F, Ding L. Modification of COF-108 via impregnation/functionalization and Li-doping for hydrogen storage at ambient temperature. *Int J Hydrogen Energy* 2017;42(16):11461–8.
- [13] Liu C, Chen Y, Wu C-Z, Xu S-T, Cheng H-M. Hydrogen storage in carbon nanotubes revisited. *Carbon* 2010;48(2):452–5.
- [14] Venkataramanan NS, Khazaei M, Sahara R, Mizuseki H, Kawazoe Y. First-principles study of hydrogen storage over Ni and Rh doped BN sheets. *Chem Phys* 2009;359(1):173–8.
- [15] Liu P, Zhang H, Cheng X, Tang Y. Transition metal atom Fe, Co, Ni decorated B₂₈ fullerene: potential material for hydrogen storage. *Int J Hydrogen Energy* 2017;42(22):15256–61.
- [16] Ren H, Cui C, Li X, Liu Y. A DFT study of the hydrogen storage potentials and properties of Na- and Li-doped fullerenes. *Int J Hydrogen Energy* 2017;42(1):312–21.
- [17] Hug S, Mesch MB, Oh H, Popp N, Hirscher M, Senker J, et al. A fluorene based covalent triazine framework with high CO₂ and H₂ capture and storage capacities. *J Mater Chem A* 2014;2(16):5928–36.
- [18] Eletskaia AV, Iskandarova IM, Knizhnik AA, Krasikov DN. Graphene: fabrication methods and thermophysical properties. *Physics-Uspekhi* 2011;54(3):227–58.
- [19] Kaur H, Yadav S, Srivastava AK, Singh N, Schneider JJ, Sinha OP, et al. Large area fabrication of semiconducting phosphorene by Langmuir-Blodgett assembly. *Sci Rep* 2016;6.
- [20] Yadav S, Tam J, Singh CV. A first principles study of hydrogen storage on lithium decorated two dimensional carbon allotropes. *Int J Hydrogen Energy* 2015;40(18):6128–36.
- [21] Wang F, Zhang T, Hou X, Zhang W, Tang S, Sun H, et al. Li-decorated porous graphene as a high-performance hydrogen storage material: a first-principles study. *Int J Hydrogen Energy* 2017;42(15):10099–108.
- [22] Kalamse V, Tavhare P, Deshmukh A, Krishna R, Titus E, Chaudhari A. Effect of boron substitution on hydrogen storage capacity of Li and Ti decorated naphthalene. *Int J Hydrogen Energy* 2017. <http://dx.doi.org/10.1016/j.ijhydene.2017.02.107>. Article in press.
- [23] Antipina LY, Avramov PV, Sakai S, Naramoto H, Ohtomo M, Entani S, et al. High hydrogen-adsorption-rate material based on graphane decorated with alkali metals. *Phys Rev B* 2012;86(8): 085435.
- [24] Dhanabalan SC, Ponraj JS, Guo Z, Li S, Bao Q, Zhang H. Emerging trends in phosphorene fabrication towards next generation devices. *Adv Sci* 2017.
- [25] Liu H, Neal AT, Zhu Z, Xu X, Tomanek D, Ye PD, et al. Phosphorene: an unexplored 2D semiconductor with a high hole mobility. *ACS Nano* 2014;8(4):4033–41.
- [26] Li L, Yu Y, Ye GJ, Ge Q, Ou X, Wu H, et al. Black phosphorus field-effect transistors. *Nat Nanotechnol* 2014;9(5):372–7.
- [27] Li Q-F, Wan XG, Duan C-G, Kuo J-L. Theoretical prediction of hydrogen storage on Li-decorated monolayer black phosphorus. *J Phys D Appl Phys* 2014;47(46):465302.
- [28] Mu Y, Si M. The mechanical exfoliation mechanism of black phosphorus to phosphorene: a first-principles study. *Europhys Lett* 2015;112(3):37003.
- [29] Kou L, Chen C, Smith SC. Phosphorene: fabrication, properties, and applications. *J Phys Chem Lett* 2015;6(14):2794–805.
- [30] Lu W, Nan H, Hong J, Chen Y, Zhu C, Liang Z, et al. Plasma-assisted fabrication of monolayer phosphorene and its raman characterization. *Nano Res* 2014;7(6):853–9.
- [31] Wei Q, Peng X. Superior mechanical flexibility of phosphorene and few-layer black phosphorus. *Appl Phys Lett* 2014;104(25):251915.
- [32] Li Q-F, Duan C-G, Wan X, Kuo J-L. Theoretical prediction of anode materials in Li-ion batteries on layered black and blue phosphorus. *J Phys Chem C* 2015;119(16):8662–70.
- [33] Ding Y, Wang Y. Structural, electronic, and magnetic properties of adatom adsorptions on black and blue phosphorene: a first-principles study. *J Phys Chem C* 2015;119(19):10610–22.
- [34] Cai Y, Ke Q, Zhang G, Zhang Y-W. Energetics, charge transfer, and magnetism of small molecules physisorbed on phosphorene. *J Phys Chem C* 2015;119(6):3102–10.
- [35] Yu Z, Wan N, Lei S, Yu H. Enhanced hydrogen storage by using lithium decoration on phosphorene. *J Appl Phys* 2016;120(2):024305.
- [36] Zhang R, Wu X, Yang J. Blockage of ultrafast and directional diffusion of Li atoms on phosphorene with intrinsic defects. *Nanoscale* 2016;8(7):4001–6.
- [37] Sun Q, Wang Q, Jena P, Kawazoe Y. Clustering of Ti on a C60 surface and its effect on hydrogen storage. *J Am Chem Soc* 2005;127(42):14582–3.
- [38] Yang S, Yoon M, Wang E, Zhang Z. Energetics and kinetics of Ti clustering on neutral and charged C₆₀ surfaces. *J Chem Phys* 2008;129(13):134707.
- [39] Kim D, Lee S, Hwang Y, Yun K-H, Chung Y-C. Hydrogen storage in li dispersed graphene with stone–wales defects: a first-principles study. *Int J Hydrogen Energy* 2014;39(25):13189–94.
- [40] Seenithurai S, Pandyan RK, Kumar SV, Saranya C, Mahendran M. Li-decorated double vacancy graphene for

- hydrogen storage application: a first principles study. *Int J Hydrogen Energy* 2014;39(21):11016–26.
- [41] Lee S, Lee M, Choi H, Yoo DS, Chung Y-C. Effect of nitrogen induced defects in li dispersed graphene on hydrogen storage. *Int J Hydrogen Energy* 2013;38(11):4611–7.
- [42] Hu W, Yang J. Defects in phosphorene. *J Phys Chem C* 2015;119(35):20474–80.
- [43] Giannozzi P, Baroni S, Bonini N, Calandra M, Car R, Cavazzoni C, et al. Quantum espresso: a modular and open-source software project for quantum simulations of materials. *J Phys Condens Matter* 2009;21(39). 395502 (19pp). URL, <http://www.quantum-espresso.org>.
- [44] Perdew JP, Burke K, Ernzerhof M. Generalized gradient approximation made simple. *Phys Rev Lett* 1996;77(18):3865.
- [45] Troullier N, Martins JL. Efficient pseudopotentials for plane-wave calculations. *Phys Rev B* 1991;43(3):1993.
- [46] Van Troeye B, Torrent M, Gonze X. Interatomic force constants including the DFT-D dispersion contribution. *Phys Rev B* 2016;93(14):144304.
- [47] Grimme S. Semiempirical GGA-type density functional constructed with a long-range dispersion correction. *J Comput Chem* 2006;27(15):1787–99.
- [48] Monkhorst HJ, Pack JD. Special points for brillouin-zone integrations. *Phys Rev B* 1976;13(12):5188.
- [49] Methfessel M, Paxton A. High-precision sampling for brillouin-zone integration in metals. *Phys Rev B* 1989;40(6):3616.
- [50] Kotakoski J, Krasheninnikov A, Nordlund K. Energetics, structure, and long-range interaction of vacancy-type defects in carbon nanotubes: atomistic simulations. *Phys Rev B* 2006;74(24):245420.
- [51] Banhart F, Kotakoski J, Krasheninnikov AV. Structural defects in graphene. *ACS nano* 2010;5(1):26–41.
- [52] Guo G-C, Wei X-L, Wang D, Luo Y, Liu L-M. Pristine and defect-containing phosphorene as promising anode materials for rechargeable li batteries. *J Mater Chem* 2015;A3(21):11246–52.
- [53] Wang J, Du Y, Sun L. Ca-decorated novel boron sheet: a potential hydrogen storage medium. *Int J Hydrogen Energy* 2016;41(10):5276–83.
- [54] Yadav S, Zhu Z, Singh CV. Defect engineering of graphene for effective hydrogen storage. *Int J Hydrogen Energy* 2014;39(10):4981–95.
- [55] Loken C, Gruner D, Groer L, Peltier R, Bunn N, Craig M, et al. Scinet: lessons learned from building a power-efficient top-20 system and data centre. *IOP Publishing J Phys Conf Ser* 2010;256:012026.